Relative intensity noise characteristics of injection-locked semiconductor lasers

X. Jin and S. L. Chuang[a)]

University of Illinois at Urbana–Champaign, Department of Electrical and Computer Engineering, 1406 West Green Street, Urbana, Illinois 61801

An experimental and theoretical study of relative intensity noise (RIN) spectra of side-mode injection-locked Fabry–Pérot semiconductor lasers is reported. It is shown that the injection-locking technique effectively increases the relaxation oscillation frequency from 4.5 GHz (free-running mode) to 12 GHz (injection-locked mode) and enhances relaxation peaks of the slave laser RIN spectra. Results from our theoretical model, which include the key parameters for semiconductor quantum-well lasers, such as the linewidth enhancement factor, the nonlinear gain saturation coefficients, and optical confinement factor, show good agreement with our experimental results. © *2000 American Institute of Physics.* [S0003-6951(00)03435-5]

Considerable attention has recently been paid to injection locking in semiconductor lasers due to the desire to develop broader-bandwidth laser systems. Several studies have predicted that the modulation bandwidth of strongly injection-locked semiconductor lasers can be significantly improved compared to the free-running case.[1,2] This is very attractive since it may allow one to achieve large modulation bandwidths with conventional semiconductor lasers at room temperature, avoiding the use of advanced devices and the need for complicated fabrication techniques. Injection locking influencing the modulation bandwidth of semiconductor lasers was shown experimentally and theoretically.[3] Simpson and Liu indirectly observed the increase of the relaxation frequency[1] and presented the noise reduction for an injection-locked laser.[4] Meng, Chau, and Wu[5] reported experimental data directly demonstrating the improvement of modulation responses. Measurements of the eye diagrams of injection-locked lasers also confirm the bandwidth improvement.[6]

However, little experimental work on the relative intensity noise (RIN) and the variation of the relaxation oscillation frequency for injection-locked semiconductor lasers are available in the literature.[4,7] Several theoretical simulations of noise characteristics have been reported,[4,8–11] with one of them predicting the relaxation frequency enhancement.[4] In this letter, we report experimental results and theoretical calculations of RIN spectra of an injection-locked Fabry–Pérot (FP) laser, and show very good agreement between the theory and experiment. We also compare the RIN spectra of the free-running laser with the injection-locked laser and show an increase of relaxation frequency from 4.5 GHz (free running) to 12 GHz (injection locked).

The experimental setup is shown in Fig. 1. The injection signal from a single-mode distributed-feedback (DFB) master laser passes through an erbium-doped fiber-optical amplifier (EDFA). The EDFA is used to amplify the pump DFB laser power and control its injection power into the slave laser over a range up to a few milliwatts. A tunable 3-nm-bandwidth optical filter is used to remove excess signals on the side modes. The injection level is monitored by an optical power meter through a 1%–99% optical coupler. The slave laser is a compressively strained InGaAsP quantum-well (QW) FP laser with a threshold of 16 mA (25 °C). The detailed structural parameters are listed in Ref. 12 as sample A. Optical isolators are used to prevent feedback. The optical signal is converted to an electrical signal using a photodetector, amplified by an 18 dB gain microwave amplifier, and measured by the electrical spectrum analyzer (HP 8593E). The optical spectra are taken by in optical spectrum analyzer (HP 70951B).

The optical spectra of (a) the free-running slave laser, (b) the master laser through the filter, and (c) the injection-locked slave laser are shown in Fig. 2. The slave laser is biased at 30 mA (25 °C) and lases at 1554.9 nm with a side-mode suppression ratio (SMSR) of 20 dB. The master laser is biased at 40 mA (21 °C), emitting at 1546.6 nm, which is close to the seventh side mode on the short-wavelength side of the free-running mode. When the master laser signal is injected into the slave laser biased above threshold, it competes with the spontaneous emission of the slave laser for amplification. When the injected signal is strong enough and close to an eigenfrequency of the slave laser, it is amplified since there is gain avaliable. At the same time, it saturates the gain of the other modes and reduces the other free-running modes. Once injection locking is fully
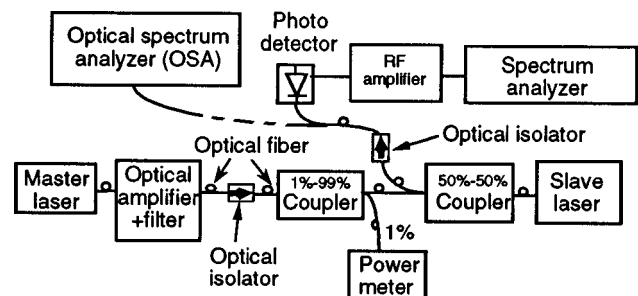

FIG. 1. Experimental setup of optical injection locking in a semiconductor (slave) laser. The master laser is a DFB laser, and the slave laser is a Fabry–Pérot quantum-well laser.

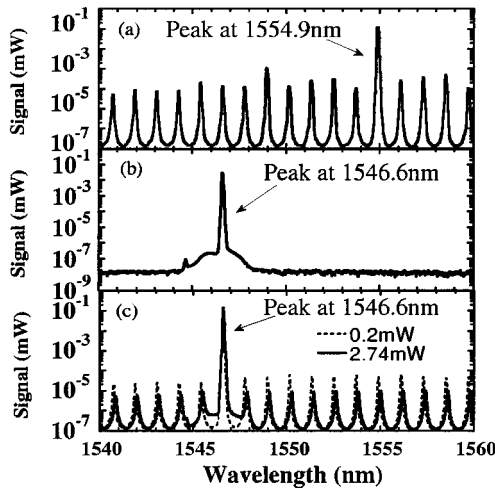[a)]Electronic mail: s-chuang@uiuc.edu

FIG. 2. Optical spectra of (a) the free-running slave laser biased at 30 mA (25 °C), (b) the master laser (DFB) at 40 mA (21 °C) with output passing through a 3 nm optical filter, and (c) the injection-locked slave laser with injection levels at 0.2 mW (dashed) and 2.74 mW (solid), respectively. The slave laser lasing wavelength switches from 1554.9 nm (free-running mode) to the master laser wavelength 1546.6 nm (locked mode) by injection locking.

reached, nearly all the power of the slave laser is emitted at the master laser wavelength, as shown in Fig. 2(c). Depending on the injection level, the injected signal saturates gain more or less strongly. Thus, injection locking improves the SMSR of the slave laser from 20 dB (free running) to 40 dB (0.2 mW injection power) and 45 dB (2.74 mW injection power). It also shifts the lasing wavelength from 1554.9 to 1546.6 nm. This intermodal injection locking can switch the information from the free-running mode to any side mode as long as the gain requirement is satisfied, which is a simple optical wavelength conversion method and very useful in dense wavelength division multiplexing (DWDM) systems.

The mesured RIN spectra of the injection-locked signal with different injection levels are shown in Fig. 3(a). The RIN spectrum of the free-running slave laser is also plotted on the same graph for comparison. The slave laser and master laser are biased at 30 mA (25 °C) and 40 mA (21 °C), respectively, to fix the detuning frequency (wavelength). Our data show that the relaxation frequency of the free-running slave laser at 30 mA bias current is 4.5 GHz. The relaxation frequency increases with increasing injection power, and reaches 12 GHz at an injection power of 2.1 mW. The RIN spectra with injection power of 0.15 and 0.22 mW are in the

transition region between the unlocked and well-locked range because their SMSRs are below 25 dB. We observe the amplitude of the relaxation peaks rise and then fall, and the RIN floor level reduces with external injection because the injected signal reduces unwanted fluctuation and feedback. Furthermore, more stimulated emissions than random spontaneous emissions occur, which greatly enhances the relaxation peaks compared to the free-running case.

A semiclassical analysis is used to analyze the RIN spectra of injection-locked lasers.[8] Noise caused by spontaneous emission and carrier generation–recombination are included in the rate equations by adding the appropriate Langevin driving terms. Our model also takes into account the master laser frequency noise, intensity noise, and the optical confinement factor of the QW laser structure.[12] The gain saturation, which is expressed as $G(n)=G_0/(1+\epsilon_0 S_0+\epsilon_i S_i)$, is also included, where ϵ_0 and ϵ_i are the nonlinear gain saturation coefficients corresponding to the slave laser signal and the injected signal. The rate equations for the slave laser field are[8]

$$\frac{d}{dt}[E(t)\exp(j\omega_0 t)]$$

$$=[j\omega_N(n)+\tfrac{1}{2}(\Gamma G(n)-\alpha_o)]E(t)\exp(j\omega_0 t)$$

$$+\frac{c}{2n_g L}E_{in}(t)\exp(j\omega_0 t), \qquad (1)$$

$$\frac{d}{dt}n(t)=-\gamma n(t)-G(n)|E(t)|^2+\frac{J}{qd}, \qquad (2)$$

where $n(t)$ is the carrier density; ω_0 is the angular optical frequency which, under the injection-locking condition, is equal to that of the master laser; $E(t)$ and $E_{in}(t)$ are the complex amplitude of the slave laser and injected field; c is the velocity of light in vacuum; L and n_g are the length and the group index, respectively; $G(n)$ and α_o are the gain and cavity loss coefficients; $\omega_N(n)$ is the resonant frequency of the Nth longitudinal mode; γ is the inverse of the carrier lifetime; J is the current density; q is the unit charge; d is the active region thickness; and Γ is the optical confinement factor. In QW lasers, the carriers and photons occupy different volumes. The total number of photons in the slave laser is $S(t)=V|E(t)|^2$, while the total number of carriers is $N(t)=\Gamma V n(t)$. V is the optical mode volume. In order to take into account noise due to spontaneous emission into the slave laser cavity, we introduce the Langevin forces $[F_{\delta S}(t), F_{\delta\varphi}(t), F_{\delta N}(t)]$ into the differential forms of the rate equations and use the truncated function and Fourier analysis techniques to obtain the power spectral density of the slave laser photons.

The results from our theoretical model are shown in Fig. 3(b). We assume the total number of photons in the slave laser is constant ($S=6\times 10^7$), which is ten times bigger than the injected signal according to our optical spectra. The injected photon number varies from zero (free running) to 8.5×10^6 and is proportional to the injection power. The gain saturation coefficients are fitting parameters ($\epsilon_0=10^{-8}$ and $\epsilon_i=10^{-7}$). The optical confinement factor and the linewidth enhancement factor are obtained from previous measurements, which are 0.15 (Ref. 12) and 1.8.[13] The master laser
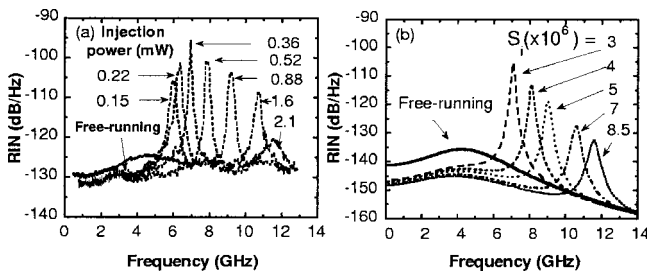

FIG. 3. RIN spectra of the injection-locked slave laser at different injection levels. (a) Experimental results of RIN with and without injection signal. At low pump levels (0.15 and 0.22 mW), the locking is incomplete. (b) Theoretical calculation of RIN spectrum of completely injection-locked and free-running lasers under different injection photon numbers.
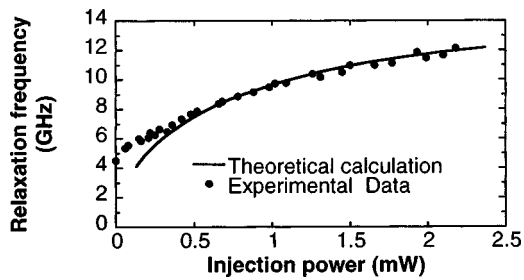
FIG. 4. Relaxation frequency vs injected power. The solid line is the theoretical calculation, and the dots are the experimental data.

signal and the slave laser signal are assumed to be in phase to simplify the calculation. Our theory shows a decrease of the RIN floor level and an enhancement of relaxation frequency with injections, which agree with the previous literature[4] and are observed in our experimental results. The injected signal reduces the cavity gain and depletes the carrier density, which decreases the spontaneous emission rate. As a result, more photons are coupled in phase into the amplified injection field and enhance the relaxation frequency. Another interesting phenomenon is that the relaxation frequency peak becomes sharper and higher with injections. This is because in the injection-locking regime, a lower injection signal directly adds photons into the slave laser cavity by using more carriers, which compensates the gain saturation and enhances the relaxation peaks of the slave laser. At stronger injections, the injected photons use up most of the available carriers, eventually saturate the signal and decrease the relaxation peaks. This is an important limit, which prevents the further improvement of the relaxation frequency.

Figure 4 shows the variation of the relaxation oscillation frequency versus injection power. The solid circles are our experimental data, and the solid line is the theoretical result. Starting at a weak injection (injection power 0.15 mW), the relaxation oscillation frequency is improved. The maximum relaxation frequency measured (12 GHz) is 2.7 times that of the free-running value (4.5 GHz). Our calculation shows good agreement with our experimental results. The deviation from the theory at weak injection levels (below 0.3 mW) comes from the incomplete locking in the experiment. It is not necessary to inject an extremely strong signal to achieve synchronization, but then the locking may not be complete. When the injection level is not high enough to saturate the

gain and extinguish all the free-running modes, our experiment leads to a bimodal behavior, and the energy is distributed between the free-running and locking mode, the latter being at the master wavelength. For this study, we limit our analysis to the complete locking regime.

In conclusion, the RIN floor of a semiconductor laser can be reduced by injection locking the slave laser with a single-wavelength master laser. We have realized an 8.3-nm-span intermodal injection locking in a FP QW laser. We have observed a 2.7 times relaxation frequency increase, and an enhancement of relaxation peaks by the injection-locking technique. For a 10 Gbit/s DWDM optical channel, a relaxation frequency of about 20 GHz is required, which is hard to achieve using a free-running laser. Injection locking is a promising method to increase the bandwidth and reduce chirp of semiconductor lasers for DWDM optical systems. Our model includes the most important features of semiconductor QW lasers, such as the linewidth enhancement factor, the nonlinear gain saturation coefficients, and the optical confinement factor. Our theoretical results agree very well with the experimental data.

[1] T. B. Simpson and J. M. Liu, IEEE Photonics Technol. Lett. **9**, 1322 (1997).

[2] J. Wang, M. K. Haldar, L. Lin, and F. V. C. Mendis, IEEE Photonics Technol. Lett. **8**, 34 (1996).

[3] O. Lidoyne, P. B. Gallion, and D. Erasme, IEEE J. Quantum Electron. **27**, 344 (1991).

[4] T. B. Simpson, J. M. Liu, and A. Gavrielides, IEEE Photonics Technol. Lett. **7**, 709 (1995).

[5] X. J. Meng, T. Chau, and M. C. Wu, Electron. Lett. **34**, 709 (1995).

[6] H. F. Chen, J. M. Liu, and T. B. Simpson, Opt. Commun. **173**, 349 (2000).

[7] Y. Hong and K. A. Shore, IEEE J. Quantum Electron. **35**, 1713 (1999).

[8] M. C. Espana-Boquera and A. Puerta-Notario, Electron. Lett. **32**, 818 (1996).

[9] G. Yabre, H. De. Wardt, H. P. A. Van den Boom, and Giok-Djan Khoe, IEEE J. Quantum Electron. **36**, 385 (2000).

[10] P. Spano, S. Piazzolis, and M. Tamburrini, IEEE J. Quantum Electron. **QE-22**, 427 (1986).

[11] N. Schunk and K. Petermann, IEEE J. Quantum Electron. **QE-22**, 642 (1986).

[12] J. Minch, S. H. Park, T. Keating, and S. L. Chuang, IEEE J. Quantum Electron. **35**, 771 (1999).

[13] T. K. J. Minch, C. S. Chang, P. Enders, W. Fang, S. L. Chuang, T. Tanbun-Ek, Y. K. Chen, and M. Sergent, IEEE Photonics Technol. Lett. **9**, 1358 (1997).